



## Spiral Embedded Electrically Small Reconfigurable Antenna

Anju Pradeep<sup>1</sup>, S Mridula<sup>1</sup> and P Mohanan<sup>2</sup>

<sup>1</sup>School of Engineering, Cochin University of Science and Technology, Kerala, India

<sup>2</sup>Department of Electronics, Cochin University of Science and Technology, Kerala, India  
anjupradeep@cusat.ac.in

### ABSTRACT

*Electrically small metamaterial antenna of zeroth order resonance incorporating a spiral resonator embedded into an asymmetric coplanar stripline is reported. The proposed antenna exhibits frequency reconfigurability of 1:1.47. The performance of the proposed antenna is compared with reported metamaterial antenna of comparable dimensions and found to be better.*

**Key words:** Electrically small antenna, reconfigurability, zeroth order antenna

### INTRODUCTION

The multi functional requirements (e.g., direction finding, beam steering, radar, control, and command) combined with space limitation place a greater challenge on today's transmitting and receiving systems. Reconfigurable antennas (RAs) are a solution to this problem. Reconfiguring of an antenna is achieved through deliberately changing its frequency, polarization, or radiation characteristics. This feat can be achieved by many techniques that alter the current paths and thus hence the fields of the antenna's effective aperture. This concept can significantly reduce the number of components and thus hardware complexity and cost of communication systems. In the early 1930s, the nulls of a two-element array were steered by using a calibrated variable phase changer in order to determine the direction of arrival of a signal [1]. The concept of 'Reconfigurability' is addressed in [2] and is defined as 'the ability to adjust beam shapes upon command'. The first patent on reconfigurable antennas was reported in 1983 by Schaubert [3]. Excellent overview of reconfigurable antennas, with many examples is given in [4-6].

Electrically reconfigurable Antennas rely on radio-frequency microelectromechanical systems (RF- MEMS), PIN diodes or varactors to redirect their surface currents [7-9]. Antennas that use photoconductive switching elements are called optically reconfigurable antennas and which make use of structure variation are called physically reconfigurable antennas. Smart materials such as ferrites and liquid crystals can also be used to achieve reconfigurability. Different categories of Reconfigurable Antennas are elaborated in [10]. They are:

- Category 1 - A radiating structure that is able to change its operating or notch frequency by hopping between different frequency bands is called frequency reconfigurable antenna [11-13].
- Category 2 - A radiating structure that is able to tune its radiation pattern is called radiation pattern reconfigurable antenna. The radiation pattern variation can be in terms of shape, direction, or gain.
- Category 3 - When a change in polarisation of antenna is caused deliberately, the structure is called polarization reconfigurable antenna. For example polarisation can shift from linear to circular polarization.
- Category 4 - Here, all changes in previous categories are combined. For example, frequency reconfiguration and polarisation diversity can be attained at the same time.

### FREQUENCY RECONFIGURABLE ANTENNA DERIVED FROM ASYMMETRIC COPLANAR STRIPLINE (ACS)

In this paper, metamaterial spiral is loaded on an ACS to achieve frequency Reconfigurable Antenna. The antenna exhibits zeroth order characteristics, making it flexible to change the dimensions without affecting the resonant frequency. Spiral in combination with microstrip transmission line exhibits CRLH property. A CRLH Transmission Line is composed of periodic repetition of CRLH unit cell of size 'p', as shown in Fig.1. The structure behaves as a uniform transmission line and may therefore be transformed into a resonator by using discontinuous (short/open) terminations.

As seen in Fig.1, the series resonance frequency is given by  $\omega_{se} = 1/\sqrt{L_R C_L}$  and shunt resonance is given by  $\omega_{sh} = 1/\sqrt{L_L C_R}$ . The case of equal series and shunt resonances is referred to as the balanced resonance condition. This is also the condition for optimal matching over a broad frequency range, hence large bandwidth. In the unbalanced resonance condition,  $\omega_{se}$  and  $\omega_{sh}$  are unequal, leading to a narrow bandwidth [14-15]. The uniplanar equivalent of a CRLH Microstrip Transmission Line may be obtained using a Coplanar Waveguide. For further size reduction, an Asymmetric Coplanar Stripline (ACS) may be used [16].

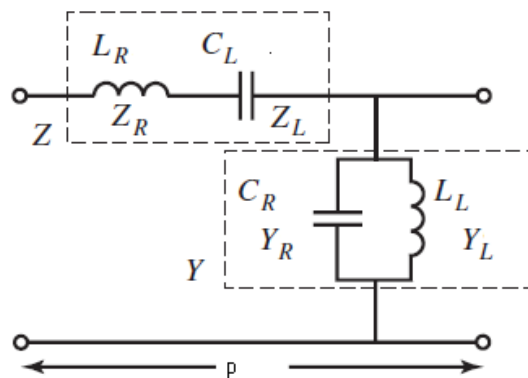


Fig.1 Equivalent circuit of CRLH Transmission Line unit cell

The evolution from spiral embedded transmission line to ACS antenna is explained below. Fig.2(a) shows an Asymmetric Coplanar Stripline of length 'L' and width 'W' corresponding to 50  $\Omega$  characteristic impedance. Width and length of ground are 'Wg' and 'Lg'. Fig. 2(b) shows spiral of length 'L' inserted between transmission line sections of length L<sub>1</sub> and L<sub>2</sub>. Fig.2(c) shows how transmission line L<sub>2</sub> is terminated in open circuit to transform the transmission line structure to ACS open ended resonator. The resonating frequency of this open ended resonator is 4.35 GHz. When a gap (gt<sub>2</sub>) of 0.2 mm is introduced between spiral and transmission line, 't<sub>2</sub>' as shown in Fig. 2(d), the resonating frequency is lowered to 2.86 GHz, due to additional capacitance. To simplify the structure of ACS, the transmission line t<sub>2</sub> is completely removed to expose a gap 'gt<sub>2</sub>' to introduce capacitance. This is shown in Fig. 2(e) and is named Type A resonator. A small short is introduced at the gap 'gt<sub>2</sub>' and is named Type B resonator. Type B resonator is shown in Fig.2 (f). From the theory of RF switches, it is well known that a PIN diode can act as open circuit in OFF condition and act as short circuit in ON condition. Hence, the short at 'gt<sub>2</sub>' is replaced by a PIN diode to switch between Type A and Type B resonators as shown in Fig. 2(g). This results in a frequency reconfigurable ACS antenna. Experimental and simulation results of this antenna are shown in Fig.2 (h). In Fig.2(g) the spiral resonator is embedded into the signal strip of a 50  $\Omega$  ACS transmission line on a substrate with  $\epsilon_r$  4.4 and thickness 1.6 mm resulting in a CRLH type antenna. The length (L<sub>1</sub>) of transmission line (t<sub>1</sub>) is optimized as 2.6 mm to achieve good matching. Width of the spiral resonator (W) is 3 mm, which is the width of the 50  $\Omega$  transmission line. The width of arms 'w<sub>1</sub>' is 0.3 mm and gap between arms of spiral 'w<sub>2</sub>' is 0.3 mm. Reduction of gap can deteriorate the antenna performance as the structure becomes more and more capacitive. The substrate dimension is optimized as 10 mm x10 mm for better impedance matching. The gap (g) between t<sub>1</sub> and ground is optimized at 0.3 mm. The width of ground (Wg) is 4 mm and length of ground (Lg) is 3.5 mm as a compromise between matching and bandwidth. When PIN diode is ON the antenna resonates at 4.35 GHz with a narrow bandwidth of 54 MHz as seen in Fig. 2(h). The input impedance of the structure at resonance is 48+j2.64 $\Omega$ . When PIN diode is OFF it introduces an additional series capacitance, reducing the resonant frequency from 4.35 GHz to 2.9 GHz as observed in Fig. 2(h). The impedance bandwidth is reduced to 40 MHz. The input impedance is 56.6-j8.43 $\Omega$  at resonant frequency, which is more capacitive. This capacitive nature of the input impedance leads to lower bandwidth [17].

Table -1 Reconfigurability by Varying Capacitance/Inductance Loading

C(pF)	Resonant Frequency (simulation) (GHz)	L(nH)	Resonant Frequency (simulation) (GHz)
short	4.35	4	4.14
2	4.66	8	3.952
5	4.52	12	3.816
7	4.488	16	3.71
10	4.472	20	3.64

A varactor diode can be used at the gap 'gt<sub>2</sub>' instead of PIN diode with varying bias voltages [18] to fine tune the resonant frequencies. Chip inductance also can be inserted at the gap (gt<sub>2</sub>) in order to fine tune resonant frequency. Variation in the simulated resonant frequency due to varying capacitor/inductor at the gap is listed in Table.1. The variation in frequency becomes minimal for inductance above 30 nH and capacitance above 10 pF.

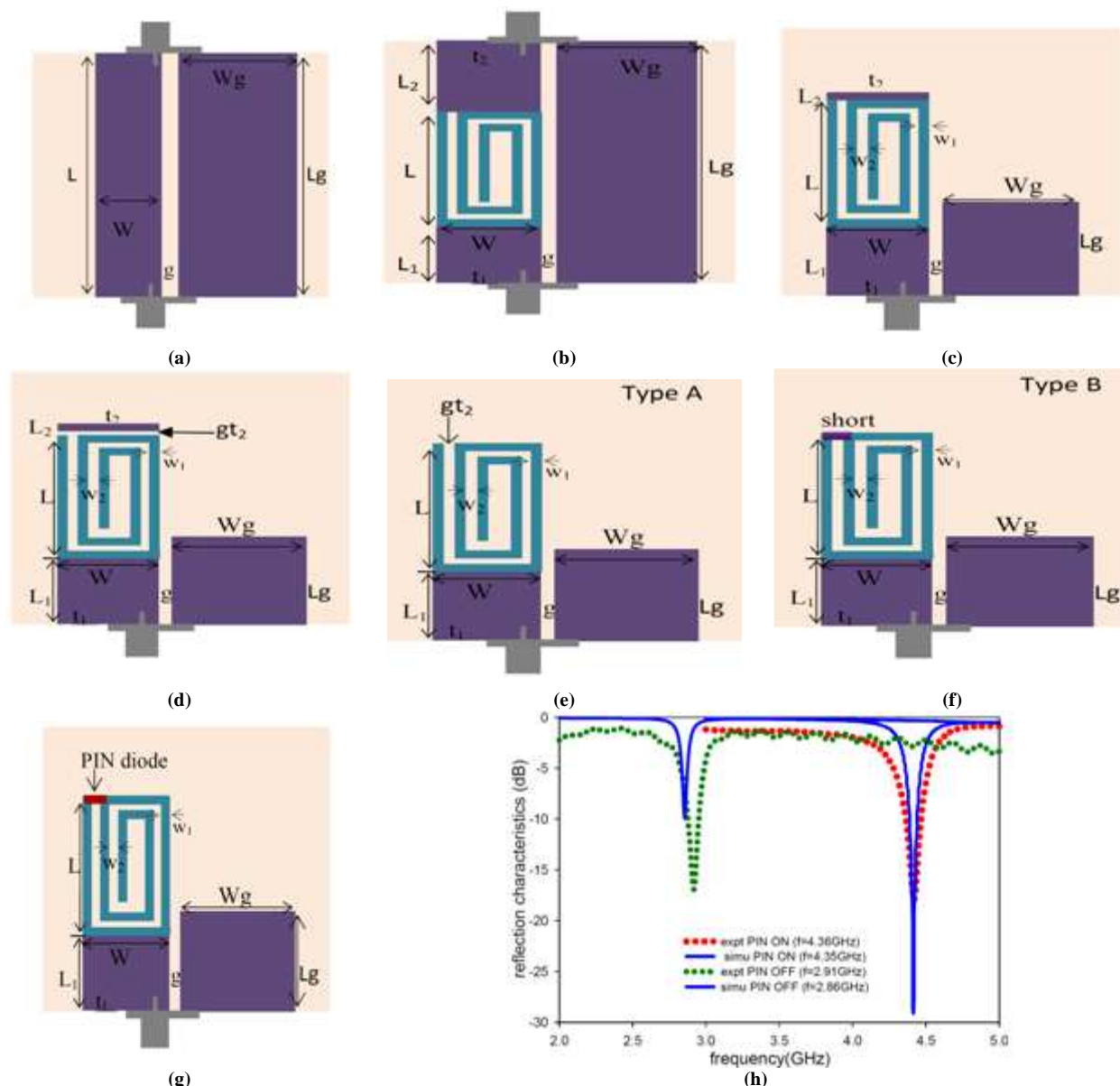


Fig. 2 (a) ACS transmission line (b) spiral embedded into ACS transmission line (c) spiral embedded ACS transmission line transformed to open ended resonator (d) gap 'gt<sub>2</sub>' introduced between t<sub>2</sub> and spiral (e) t<sub>2</sub> completely removed to yield Type A ACS (f) gap 'gt<sub>2</sub>' shorted to get Type B ACS antenna (g) PIN diode at gt<sub>2</sub> to achieve frequency reconfiguration L<sub>1</sub>=2.6mm, L=4.7mm, W=3mm, w<sub>1</sub>=0.3mm, w<sub>2</sub>=0.3mm, Wg=4mm, Lg=3.5mm, g=0.3mm (h) reflection characteristics of frequency Reconfigurable ACS antenna

### ZEROTH ORDER RESONANT ANTENNA

CRLH can exhibit zeroth order resonant (ZOR) mode in which the resonant frequency is independent of the number of unit cells. Hence, ZOR antenna is also known as infinite wavelength resonant antenna. The phase constant  $\beta = 0$  at resonant frequency implies the infinite guided wavelength  $\lambda_g = 2\pi/|\beta| = \infty$ , and zero phase shift  $\theta_m = -\beta l = 0$ . This phenomenon enables the realization of zeroth-order resonance in which the length of the resonator is independent of the resonance condition (i.e. the multiple of the half wavelength in case of the open circuited TL) [19]. For a CRLH resonator with N unit cells, its resonance occurs when

$$\beta_n = \frac{m\pi}{l} (m = 0, \pm 1, \pm 2 \dots \pm (N-1)) \tag{1}$$

where  $l = N \cdot p$  is the size of resonator and 'm' is the mode number. Hence, a CRLH resonator with N unit cells exhibits finite '2N-1' resonance frequencies. At m=0, the mode is termed as zeroth-order resonance mode and corresponds to an infinite wave-length and therefore field distribution is flat. In the unbalanced CRLH case, the zeroth order resonance corresponds to either  $\omega_{se}$  due to the short ended structure or  $\omega_{sh}$  due to the open ended structure. The active immittance elements for  $\omega_{se}$  are  $L_R - C_L$  and for  $\omega_{sh}$  is  $L_L - C_R$  (Fig.1). In the case of open ended structure, only shunt elements are active and therefore one of the series elements ( $L_R$ ) is sufficient to couple the shunt resonators of additional unit cells. Under this condition all CRLH equations are simplified by the substitution

$C_L$  tends to infinity. No more LH branch exists and only the resonance  $\omega_{sh}$  appears in the spectrum. If the size of the structure is enlarged by adding more unit cells, the resonant frequency remains the same at  $\omega_{zor} = \omega_{sh}$ . Since the resonant frequency of ZOR is independent of size, it can be enlarged by adding more unit cells to attain a very large electrical size and high directivity. The zeroth order status of Type B antenna is verified and shown in Fig.3. In order to facilitate the switching action between second order Type A and Type B antennas, the second order antenna structure is modified by placing the spiral and its mirror image laterally as shown in Fig.3(b). From Fig.3(c), it is clear that the experimental resonance frequency is almost the same for one unit cell (2.93 GHz) and for two unit cells (3.01 GHz). An extremely useful and unique property of CRLH metamaterial structures is that the size and gain can be controlled independent of the resonant frequency of the antenna.

**DISPERSION CHARACTERISTICS OF DEVELOPED ZEROth ORDER ANTENNAS**

The dispersion characteristic of the Type B antenna is shown in Fig. 4. This curve is plotted based on Floquet theorem. The antenna is first converted to a two port network by adding a small strip of transmission line at the far end, to which the second port is connected (Fig.2 (b)). Reflection and transmission characteristics are observed and the S-matrix is transformed to ABCD matrix whose eigen values give the dispersion characteristics.

$$\begin{matrix} s_{11} & s_{12} \\ s_{21} & s_{22} \end{matrix} \rightarrow \begin{matrix} A & B \\ C & D \end{matrix} \rightarrow [Eigen\ vector] \rightarrow [\gamma] \rightarrow [\beta]$$

The dispersion characteristics shows that phase is zero at the resonant frequency of Type B antenna. This indicates the zeroth order nature of the antenna. Similar result is obtained for Type A antenna also.

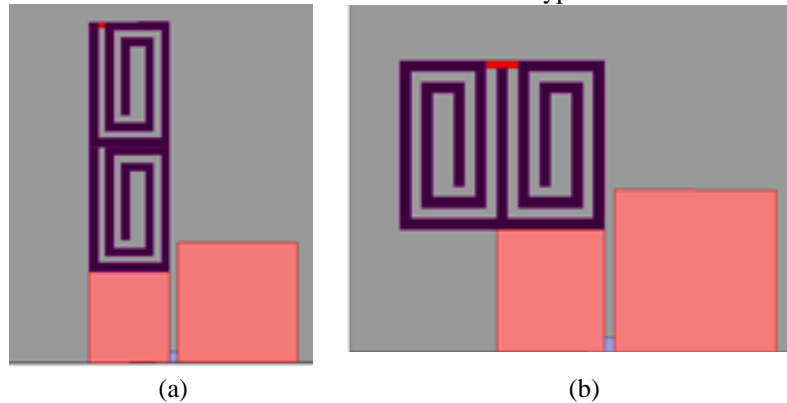


Fig. 3 (a) Spiral ACS Antenna Type B with two unit cells arranged one over the other (b) Spiral ACS Antenna Type B with two unit cells arranged side by side (c) reflection characteristics showing zeroth order response

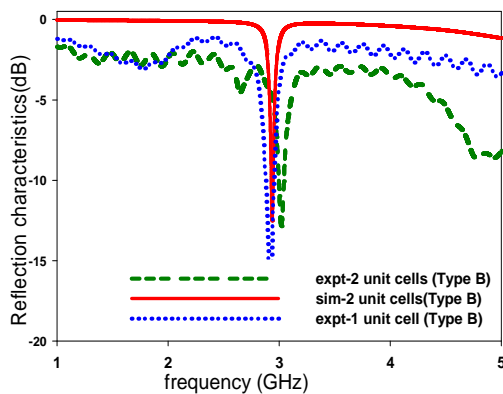


Fig. 3 (c) reflection characteristics showing zeroth order response

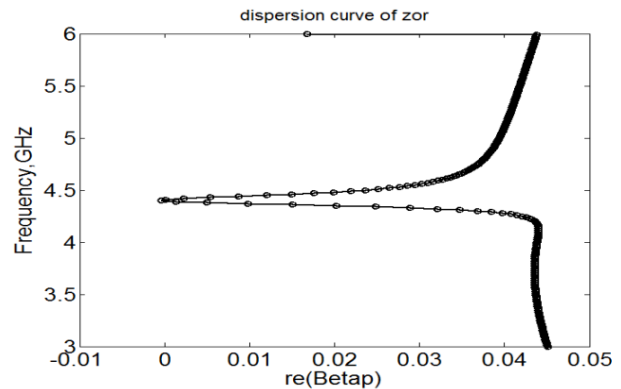


Fig. 4 Dispersion characteristic of Type B antenna proving Zeroth order nature;  $L_1=2.6\text{mm}$ ,  $L=4.7\text{mm}$ ,  $w_2=0.3\text{mm}$ ,  $Wg=4\text{mm}$ ,  $Lg=3.5\text{mm}$ ,  $g=0.3\text{mm}$ ,  $W=3\text{mm}$ ,  $w_1=0.3\text{mm}$

**PARAMETER EXTRACTION OF ACS ANTENNA**

The inductor and capacitor values are extracted using equations as follows

$$L_R = 0.5 \text{ Im } (Z') \text{ at } \omega_{se}; \tag{2}$$

$Z'$  is the first derivative with respect to  $\omega$

$$C_R = 0.5 \text{ Im } (Y') \text{ at } \omega_{sh} \tag{3}$$

$$C_L = 1/(\omega_{se}^2 L_R)$$

and

$$L_L = 1/(\omega_{sh}^2 C_R) \tag{4}$$

Since, the CRLH TL considered is lossy from experimental results, series resistance and shunt conductance are also extracted as  $R = \text{Re}(Z)$  at  $\omega_{se}$ ; and  $G = \text{Re}(Y)$  at  $\omega_{sh}$ . The values are tabulated in Table-2. From the theory of

open ended CRLH resonators, it is expected that Type A and Type B antennas would resonate at  $\omega_{sh}$ . This is verified by calculating the series and shunt resonant frequencies using equation 5 and  $\omega_{se} = \frac{1}{\sqrt{L_R C_L}}$  results are summarised in  $\omega_{sh} = \frac{1}{\sqrt{L_L C_R}}$  Table 3.

**Table - 2 Extracted Component Values of CRLH ACS Antennas**

Type of ACS	$L_R$ (nH)	$C_R$ (pF)	$L_L$ (nH)	$C_L$ (pF)	$R$ ( $\Omega$ )	$G$ ( $\Omega^{-1}$ )
Type A	2.0253	1.91	1.706	2.073	40.17	0.0716
Type B	1.086	0.128	8.56	1.203	23.84	0.0044

**Table-3 Comparison of resonant frequencies of Type A and B ACS antennas**

Type of ACS	Series resonance $\omega_{se}$ (GHz)	Shunt Resonance $\omega_{sh}$ (GHz)	Simulated Resonant Frequency (GHz)	Experimental Resonant Frequency (GHz)
A	2.4571	2.7829	2.86	2.91
B	4.405	4.428	4.35	4.36

It is clear from Table.3 that both antennas are resonating at  $\omega_{sh}$  as expected and bandwidth of Type A (from Fig.2(h)) is lower due to unbalanced nature of its resonance ( $\omega_{se} \neq \omega_{sh}$ ). Fabricated antennas are shown in Fig.5.

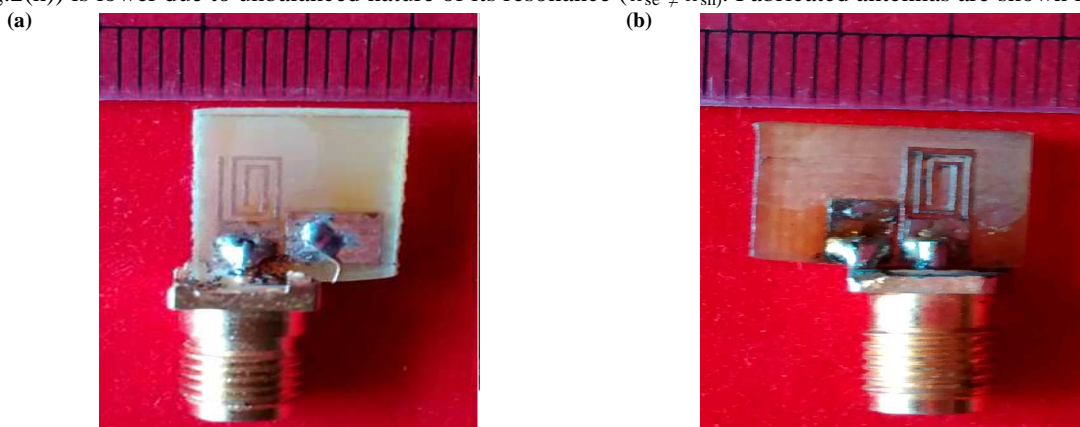


**Fig. 5 Fabricated antennas (a) Type A (b) Type B**

### RADIATION PATTERN

The radiation pattern of Type B is similar to a dipole as shown in Fig. 6(a). However, the pattern is tilted due to the asymmetric feed. Type A antenna radiates with directional characteristics as shown in Fig. 6(b). In second order arrangement, since spirals are connected back to back, directive nature of Type A is reformed to omnidirectional pattern as seen in Fig.6(c). Front to back ratio for both Type A and Type B is 1.1 for second order. Both antennas exhibit linear polarization. There is minimal variation in the radiation characteristics of Type A and Type B antennas in second order configuration, which enhances the reconfigurable nature of the proposed antenna. The radiation pattern tilt can be resolved using a CPW feed, provided there is no constraint on the size of the antenna. Simulated gain of Type B antenna is 0.146dBi and 0.186dBi for first and second orders, whereas Type A exhibits a low gain of 0.059dBi in both cases, but there is an improvement in radiation characteristics for second order compared to first order of Type A. The simulated radiation efficiency of second order Type A is 11% and second order Type B is 12.8%, which is reasonable among conventional CRLH antennas. The antenna has an added advantage of size reduction as it satisfies the condition for Electrically Small Antennas (ESA) for the two operating frequencies compared to conventional ACS monopoles [20].

### ELECTRICALLY SMALL ANTENNA (ESA)

An antenna is considered to be an Electrically Small Antenna (ESA), if  $ka = 2\pi a / \lambda_0 \leq 0.5$ , where  $k$  is the wave number, 'a' is the radius of smallest sphere that surrounds the antenna system and  $\lambda_0$  is the wavelength at resonance [21]. Most often, antenna itself is a capacitor or inductor and it is tuned to resonance by a reactor of opposite kind. For Electrically Small Antennas, the propagating modes are replaced by evanescent modes with high Q, where Q is inversely proportional to cube of radius of sphere enclosing the antenna. In short, maximum dimension enclosed within a sphere of radius 'a' regulates the maximum bandwidth of an electrically small antenna.

The difficulties encountered in the design of an electrically small antenna include:

- impedance matching
- high current density flowing on a non-perfect conductor causes insertion loss, resulting in joule heating and
- a small radiation aperture with low radiation efficiency.

The primary issues faced by Electrically Small Antennas which are very desirable for both military and commercial applications are usually directivity (gain) versus aperture size and bandwidth versus volume (Chu limit). Electrically small antennas are known to be inefficient radiators due to the relative magnitudes of the radiation and ohmic loss resistances [22]. It is concluded that size can only be reduced at the expense of bandwidth or efficiency. In general, the best performance from ESA will be achieved if the dielectric constant is as low as possible and the aspect ratio, which is the ratio of maximum to minimum dimension of antenna volume, is close to unity. The internal structure of the antenna is also such that the fields fill the minimum size enclosing the sphere with the greatest possible uniformity. Since the reflection characteristics is considered insufficient to describe the performance of an ESA, the product of bandwidth and efficiency, 'Bη' is often chosen as parameter for comparison, where B is the 3 dB bandwidth and 'η' is the efficiency. Since impedance matching is difficult, ESAs tend to be lossy. The parameter 'Bη' is sufficient for characterization of small antennas because the increase of bandwidth due to loss is met at the expense of loss in radiation efficiency. Thus the product 'Bη' gives the measure of performance for a lossy as well as lossless ESA.

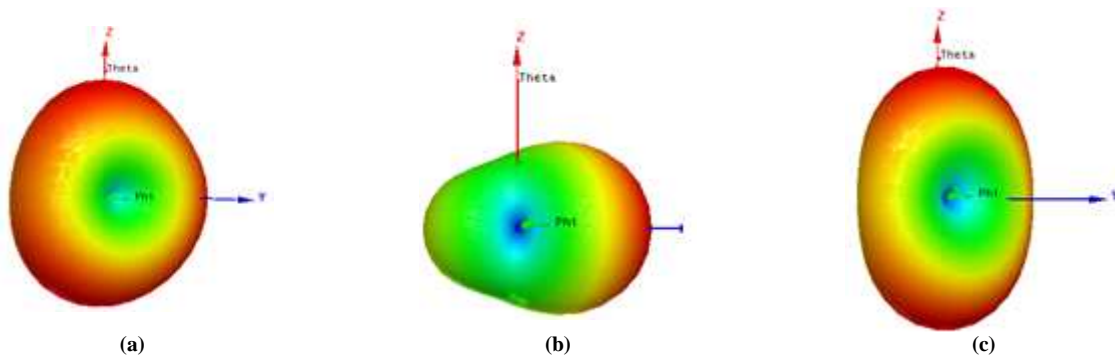


Fig. 6 (a) Radiation pattern of Type B (b) radiation pattern of Type A antenna (c) radiation pattern of second order Type A and Type B antennas

Gustaffson's limit for aspect ratio 6.25 is 0.15

Wheeler Chu limit for  $\epsilon_r = 4.4$  is 0.2

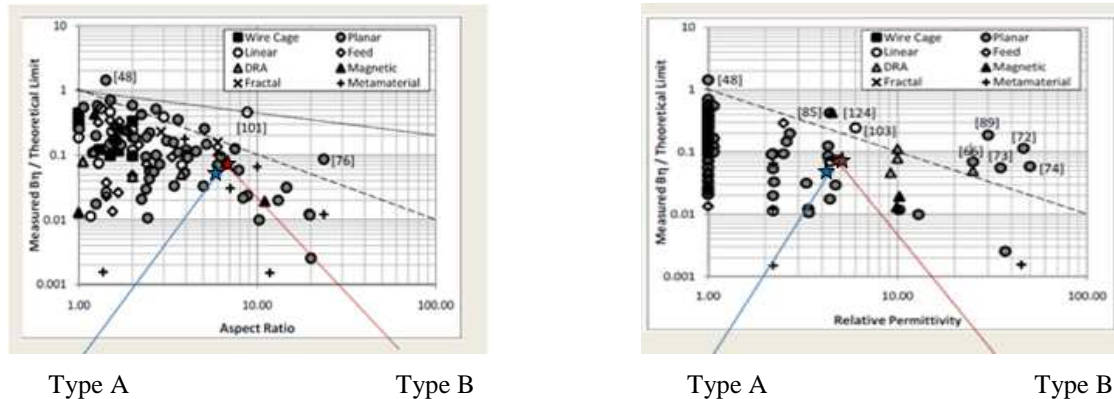


Fig. 7 Comparison of Type A and Type B antennas with respect to [23]

For Type A antenna and Type B antenna, 'ka' is found to be 0.33 and 0.47 satisfying the condition for ESA. A number of ESAs falling under different categories are compared in [23]. Comparison of the antennas discussed in this paper is also done using this approach.

The drawback of the developed antenna is its small gain. However the antenna satisfies Chu limit and has a better performance in comparison with other reported metamaterial antennas of similar size with respect to aspect ratio and substrate used for fabrication [23]. The aspect ratio is defined as the ratio of maximum to minimum dimension (the ratio of length to height of substrate) of antenna volume. The internal structure of the antenna is also such that the fields fill the minimum size enclosing the sphere with the greatest possible uniformity. Aspect ratio of developed ACS antennas is 6.25. 'Bη' is calculated for first order Type A and Type B antennas and compared with Wheeler's limit defined for a particular substrate and Gustaffson limit defined for a particular aspect ratio.  $B\eta$  (simulated) =  $0.057 \times 0.076 = 0.00433$ ; where  $B = 0.057$  is the measured bandwidth and  $\eta = 0.076$  is the simulated efficiency.  $B\eta$  (theoretical) =  $0.054 \times 1 = 0.054$ ; where  $B = 0.054$  is the simulated bandwidth and  $\eta = 1$  is the theoretical efficiency. The ratio of  $B\eta$  (simulated) to  $B\eta$  (theoretical) is 0.08, which is better than other reported metamaterial antennas [23] for a dielectric constant of 4.4. The Wheeler's limit [ratio of  $B\eta$  (measured) to  $B\eta$  (theoretical)] for this substrate is 0.2 [23]. The comparison of both antennas with respect to [23] is shown in Fig.7.

## CONCLUSION

The developed antenna is compact and coplanar with dimensions 10mm x 10mm x 1.6mm. It exhibits a frequency reconfiguration of 1.47:1. The radiation characteristics of this antenna in second order remain essentially unaffected by the frequency tuning, whereas first order can exhibit both frequency as well as radiation characteristics reconfigurability. The spiral determines the resonant frequency and hence tuning parameters are length of spiral, number of turns, width of each arm and the gap between arms. Due to its small size, it falls under the category of Electrically Small Antennas. Comparison of both antennas with respect to Wheeler Chu and Gustafsson limits reveal satisfactory performance. The small gain and efficiency may be attributed to the inherent characteristics of ESAs. However, it can be improved by designing proper matching circuits. Type A and Type B antennas also exhibit zeroth order characteristics as seen through the calculated dispersion characteristics. The zeroth order characteristics open up possibility for performance enhancement without varying frequency. The highly reactive and intense near field of these metamaterial ESAs can be utilized for near field applications like sensor networks. The sensitivity of microwave networks is inversely proportional to its order of resonance. Thus the proposed antenna is predicted to have very high sensitivity making it an ideal candidate for sensor applications by virtue of its zeroth order nature and electrically small size.

## REFERENCES

- [1] HT Friis, CB Feldman and WM Sharpless, The Determination of the Direction of Arrival of Short Radio Waves, *Proceedings of the Institute of Radio Engineers*, **1934**, 22 (1), 47-78.
- [2] EW Matthews, CL Cuccia and MD Rubin, Technology Considerations for the Use of Multiple Beam Antenna Systems in Communications Satellites, *IEEE Trans on Microwave Theory and Techniques*, **1979**, 27, 998-1004.
- [3] D Schaubert, *Frequency-Agile Polarization Diversity Microstrip Antennas and Frequency Scanned Arrays*, US Patent -4367474, **1983**.
- [4] JT Bernhard, *Reconfigurable Antennas*, San Rafael, CA, USA, Morgan & Claypool Publishers, **2007**.
- [5] Christos G Christodoulou, Youssef Tawk, Steven A Lane and Scott R Erwin, Reconfigurable Antennas for Wireless and Space Applications *Proceedings of the IEEE*, **2012**, 100(7), 2250-2261.
- [6] RL Haupt and M Lanagan, Reconfigurable Antennas, *IEEE Antennas and Propg Magazine*, **2013**, 55 (1), 49-61.
- [7] Chapter 1: Understanding Key RF Switch Specifications, *The Guide to Selecting an RF Switch*, National Instruments, **2011**.
- [8] Solid State Switches, *Microwave Encyclopaedia*, **2010**.
- [9] The PIN Diode Circuit Designers, *Microsemi Corporation Handbook*, Microsemi Corporation California, USA, **1998**.
- [10] J Costantine, *Design, Optimization and Analysis of Reconfigurable Antennas*, New Mexico University (UNM), Albuquerque, New Mexico, **2009**.
- [11] Y Cai, YJ Guo and TS Bird, A Frequency Reconfigurable Printed YAGI-UDA Dipole Antenna for Cognitive Radio Applications, *IEEE Transactions on Antennas and Propagation*, **2012**, 60 (6), 2905-2912.
- [12] Dimitrios Peroulis, Kamal Sarabandi and Linda PB Katehi, Design of Reconfigurable Slot Antennas, *IEEE Transactions on Antennas and Propagation*, **2005**, 53 (2), 645-654.
- [13] Chang Yong Rhee, Jea Hak Kim, Woo Jae Jung and Taejoon Park, Frequency-Reconfigurable Antenna for Broadband Airborne Applications, *IEEE Antennas and Propagation Letters*, **2014**, 13, 189-192.
- [14] Christophe Caloz and Andre Renning S, Overview of Resonant Metamaterial Antennas, *European Conference on Antennas and Propagation*, Berlin, Germany, **2009**, 615-619.
- [15] Filippo Capalino, *Metamaterials Handbook- Applications of Metamaterials*, CRC Press, USA, **2009**.
- [16] V Deepu, R Sujith, S Mridula, CK Aanandan, K Vasudevan and P Mohanan, ACS Fed Printed F-Shaped Uiplanar Antenna for Dual Band WLAN Applications, *Microw and Optical Tech Letters*, **2009**, 51 (8), 1852-1856.
- [17] Filiberto Bilotti, Alessandro Toscano and Lucio Vegni, Equivalent-Circuit Models for the Design of Metamaterial Based on Artificial Inclusions, *IEEE Transactions on Microwave Theory and Techniques*, **2007**, 55 (12), 2865-2873.
- [18] Christophe Caloz and Tatsuo Itoh, *Electromagnetic Metamaterials: Transmission Line Theory and Microwave Applications - The Engineering Approach*, John Wiley & Sons Inc., New Jersey, **2006**.
- [19] A Andreone, A Cusano, A Cutolo and V Galdi, *Selected Topics in Photonic Crystals and Metamaterials*, World Scientific Publishing Co. Pvt.Ltd, Singapore, **2011**, 202-205.
- [20] LJ Chu, Physical Limitations of Omnidirectional Antennas, *Journal of Applied Physics*, **1948**, 19(12), 1163-1175.
- [21] HA Wheeler, The Radian Sphere Around a Small Antenna, *Proceedings of the IRE*, **1959**, 47, 1325-1331.
- [22] Gary A Thiele, Phil L Detweiler and Robert P Penno, On the Lower Bound of the Radiation Q for Electrically Small Antennas *IEEE Transactions on Antennas and Propagation*, **2003**, 51(6), 1263-1269.
- [23] Daniel Sievenpiper, David Dawson and Minu Jacob, Experimental Validation of Performance Limits and Design Guidelines for Small Antennas, *IEEE Transactions on Antennas and Propagation*, **2012**, 60 (1), 18-19.